Supplementary material

Neural basis of cognitive control over movement inhibition: human fMRI and primate electrophysiology evidence

Figure S1. Related to Figure 2: Primate behavioral results for the context-dependent SST. A) Inhibition function and Continue function for one exemplar behavioral session. The black circles show raw inhibition function, and the black line shows weibull-fitted inhibition function. The black diamonds show raw Continue function. **B)** Mean reaction time in Go (grey), Failed Stop (black), and Continue (white) trials. **C)** Mean Stop signal reaction time (SSRT, black) and Continue signal reaction time (CSRT, white). Error bars indicate the standard error of the mean.

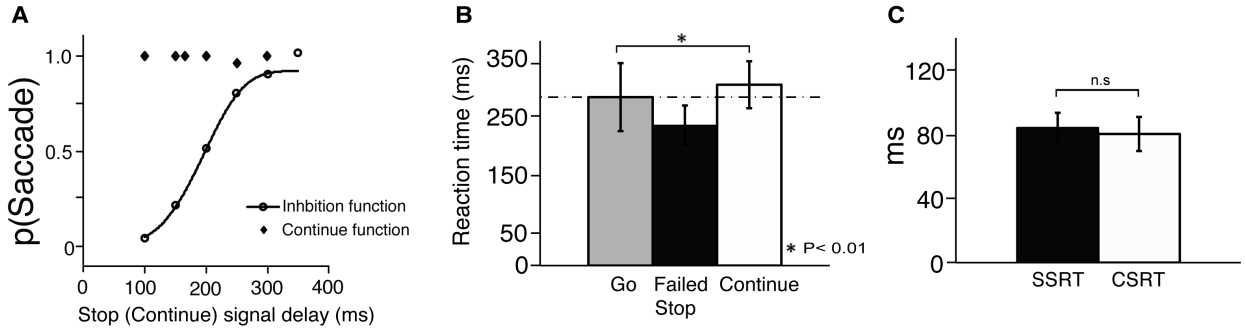

Figure S2. Related to Figure 2: Example cumulative distribution functions of reaction times Illustrating the new Modified Integration method for calculating SSRT and CSRT for each participant. Top panels, data from one human participant. Bottom panels, data from one behavioral session in the monkey. **A.** Stop trial reaction time distributions relative to Stop signal onset from Stop trials (colored) and yoked (re-aligned) Go trials (mean, dotted black; 99.9% CI, solid black). The intersection of Stop trials and the upper 99.9% CI bound (solid black) defined an optimal Stop signal reaction time cutoff (magenta vertical dashed line) that best separated Failed Stop (red line) and Successful Stop (blue line) trials. **B.** Continue trial reaction time distributions relative to Continue signal onset from Continue trials (colored) and yoked Go trials (mean, dotted black; 99.9% CI, solid black). The intersection of Continue trials and the 99.9% CI bound (solid black) defined an optimal Continue signal reaction time cutoff (magenta vertical dashed line) that best separated Fast Continue (red line) and Slow Continue (blue line) trials. Human data shown are for illustrative purposes from one individual who participated in a different experiment in which context did not switch across blocks, resulting in twice as much data to fit the CDF. For further data from that experiment and more extensive behavioral analysis of the task, see Xu et al. (Under review/revision). Also see Mayse et al. (2014).

HUMAN

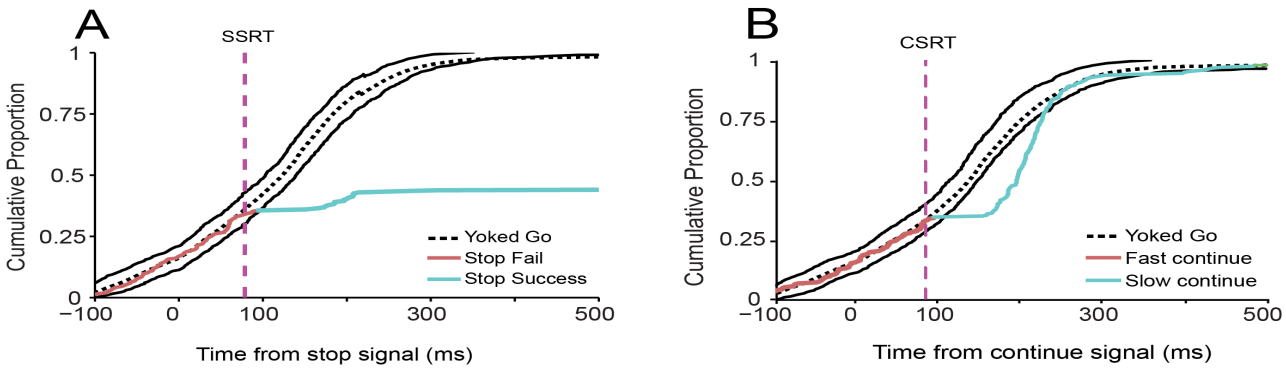

MONKEY

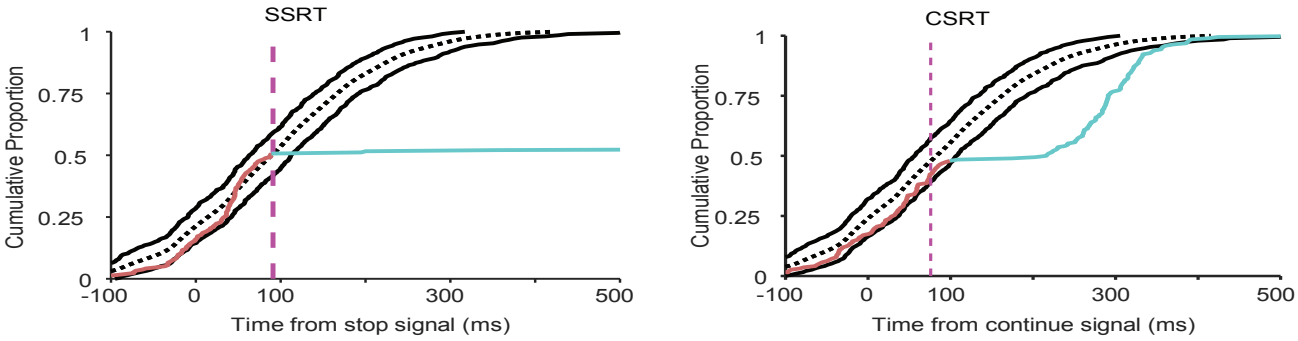

Figure S3. Related to Figures 5 & 6: Dorsal view of primate electrophysiology recording site with neural functional classification. A total number of 326 rVLPFC neurons were recorded and 313 (96%) showed task related activity. Of the 313 neurons, 37 (11.8%) neurons were with saccade related activity, 15 with visual related activity (4.8%), 48 (15.3%) with visual-movement related activity and 196 (62.6%) with context-related activity. The response of 196 neurons with context-related activity can be further broken down into context-dependent visual (n=15), context-dependent saccadic (n=47), context-dependent postsaccadic (n=86), and context-dependent reward (n=4) related activity; the remaining 39 neurons exhibited stimulus driven context related activity that increased firing rate on switch trials, where a new context replaced the old context. Mov: neurons shown movement-related activity. Vis: neurons shown visual-information-related activity. VM: neurons show both movement and visual information related activity. Fix: neurons shown fixation-related activity. Ctx: neurons shown context-related activity. PS: principle sulcus. AS: arcuate sulcus. CS: central sulcus. Red hexagon illustrates the recording chamber.

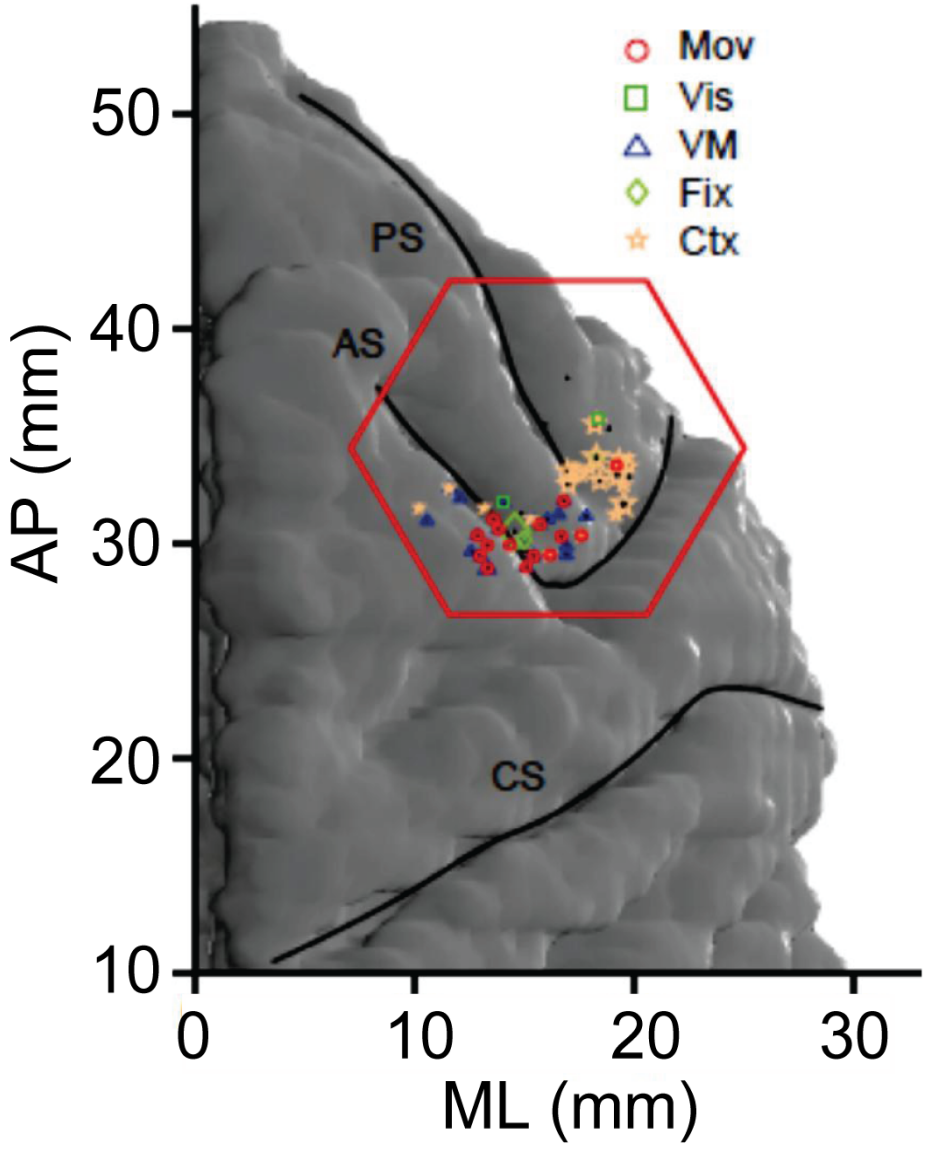

Figure S4. Related to Figures 5&6: Primate electrophysiology recording sites. A dorsal view of the brain for the monkey reconstructed from the MRI showing the locations of neurons recorded in the frontal eye field (blue diamonds), area 46 (teal triangles), and area 45 (red squares). Neuronal classification was based on both the functional properties and anatomical location of the neurons. The red hexagon indicates the limits of the recording chamber.

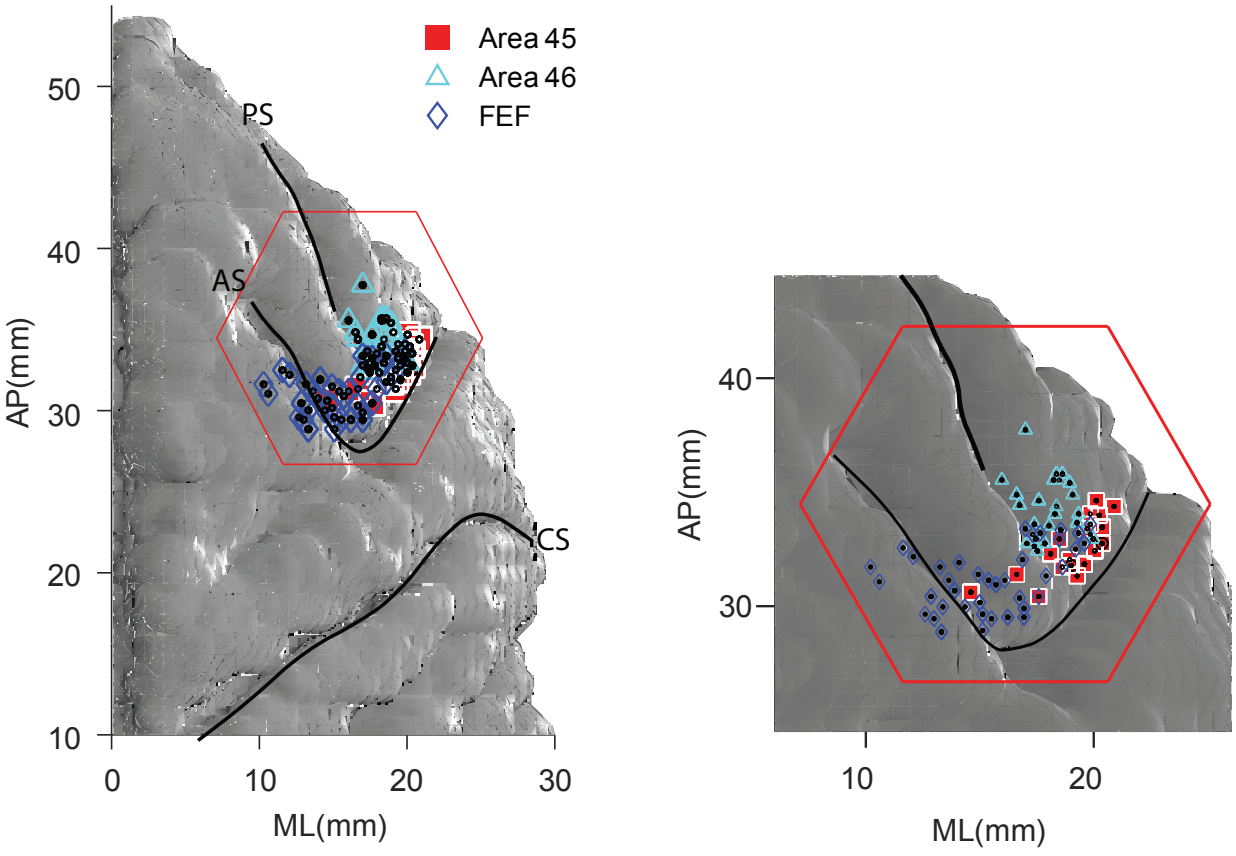

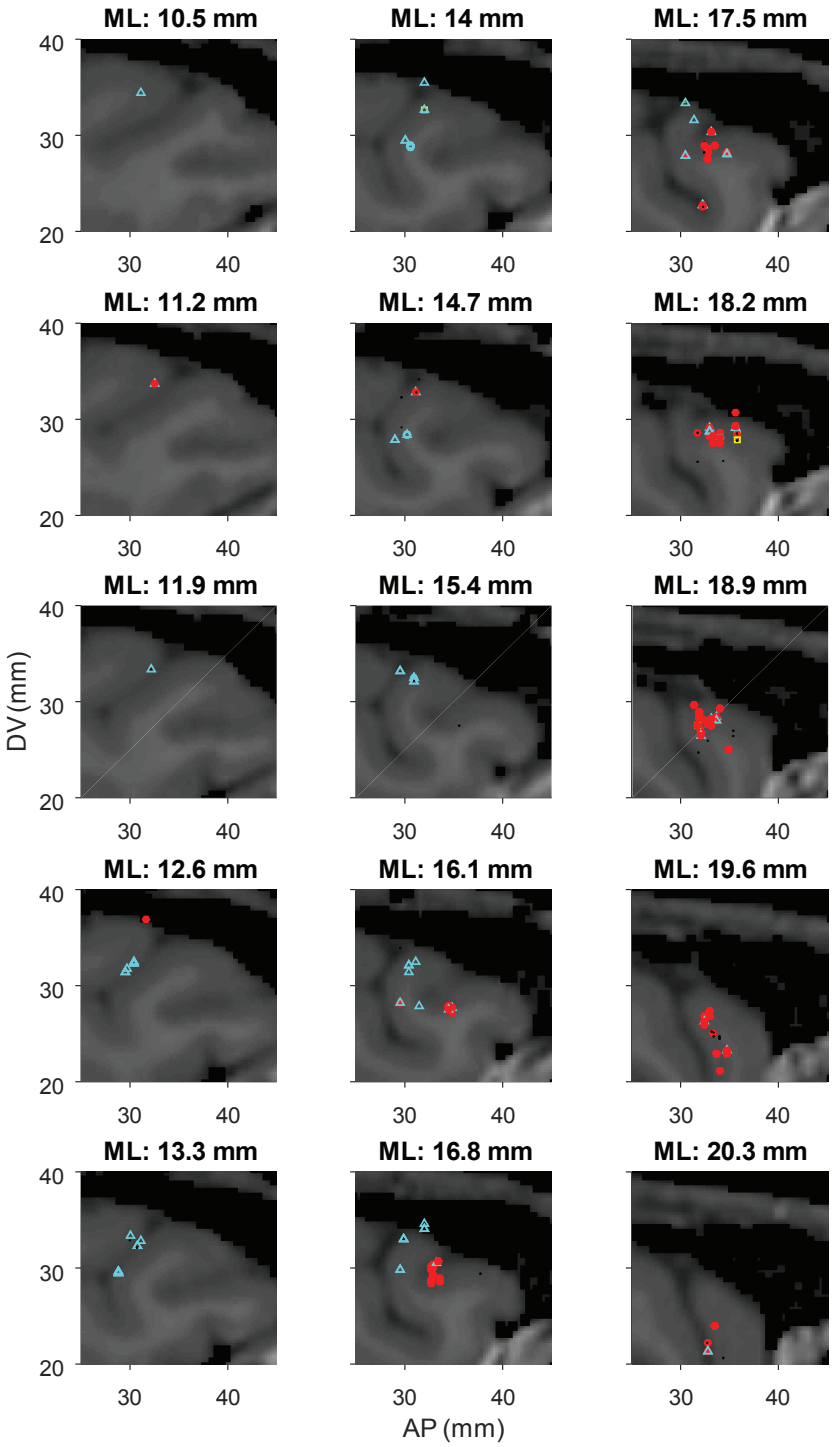

Figure S5. Related to Figures 5 & 6: Parasagital MRI sections for monkey reconstructed from the MRI showing the locations of neurons recorded in the frontal cortex. Neuronal classification was based on both the functional properties and anatomical location of the neurons. The teal triangles indicate sites where the activity of neurons with visual or movement related activity was acquired. The red squares indicate sites where the activity of neurons with context related activity was acquired. Black dots indicate sites where no task related activity was observed.

Table S1. Human fMRI Results. Related to Figure 3. Regions demonstrating greater activation for Successful Stop compared with Go trials.

Area	Talairach coordinates (mm)			Volume
	x	y	z	(mm^3)
R ventrolateral prefrontal cortex/insula	33	21	6	2,502
R inferior parietal lobule	37	-59	44	1,806
L claustrum	-27	21	10	831
L inferior frontal lobule	-33	-51	38	633
R cingulate gyrus	7	21	34	366
R caudate	11	7	6	268
R superior parietal lobule	15	-65	34	197
L caudate	-11	1	14	184
L precentral gyrus	-41	-1	36	119
R thalamus	13	-11	4	91

Note. Talairach coordinates indicate the peak voxel within each cluster (family-wise error, $p < .05$). R, right; L, left; B, bilateral.

Table S2. Human fMRI Results. Related to Figure 3. Regions demonstrating greater activation for Failed Stop compared with Go trials.

Area	Talairach coordinates (mm)			Volume
	x	y	z	(mm^3)
R ventrolateral prefrontal cortex/insula	41	21	4	2,044
R inferior parietal lobule	33	-55	40	947
L claustrum	-27	21	10	500
L inferior frontal lobule	-33	-51	38	633
L cingulate gyrus	-7	-31	30	425
R superior frontal gyrus	3	17	50	314
L inferior frontal lobule	-33	-53	38	265
R middle temporal gyrus	55	-41	4	92
R precentral gyrus	15	-65	32	88

Table S3. Human fMRI Results. Related to Figure 3. Regions demonstrating greater activation for Stop trials compared with Go trials.

Area	Talairach coordinates (mm)			Volume (mm^3)
	x	y	z	
R ventrolateral prefrontal cortex	39	3	30	2,589
R angular gyrus	33	-55	38	1,775
L claustrum	-27	21	10	749
R superior frontal gyrus	5	15	48	473
L angular gyrus	-31	-53	38	452
L cingulate gyrus	-5	-31	30	391
R superior parietal lobule	15	-65	34	170
R caudate	13	11	4	160
L caudate	-9	5	10	111
L precentral gyrus	-37	1	28	100

Table S4. Human fMRI Results. Related to Figure 3. Regions demonstrating greater activation for Continue trials compared with Go trials.

Area	Talairach coordinates (mm)			Volume (mm^3)
	x	y	z	
R superior parietal lobule	39	-65	44	1,371
R ventrolateral prefrontal cortex	39	-1	30	1,054
L inferior parietal lobule	-35	-53	40	909
L inferior frontal gyrus	-37	1	30	417
L superior frontal gyrus	-3	13	48	220
L insula	-37	11	10	205
R insula	39	15	4	198
L cingulate gyrus	-3	-33	30	163
R superior parietal lobule	9	-69	36	159
L middle frontal gyrus	-41	27	26	117

Table S5. Human fMRI connectivity results. Related to Figure 7. Regions demonstrating greater connectivity with the seed region, during Stop trials, compared with baseline.

Area	Talairach coordinates (mm)			Volume
	x	y	z	(mm^3)
Seed: ventral rVLPFC				
L superior parietal lobule	-7	-49	46	1,001
L frontal eye field	-27	-7	48	565
L superior frontal gyrus	-3	15	50	278
L insula	-31	15	4	170
L putamen	-15	11	4	159
R frontal eye field	31	11	48	146
R cingulate gyrus	1	-41	30	135
R superior temporal gyrus	45	-57	14	92
L superior temporal gyrus	-53	-47	12	91
Seed: dorsal rVLPFC				
L Caudate	-19	-13	20	375
R Caudate	15	-11	20	348
L precentral gyrus	-51	9	10	346
R medial frontal gyrus	7	45	34	313
L superior temporal gyrus	-47	-23	5	222
L ventrolateral al prefrontal cortex/ inferior frontal gyrus	-45	37	4	171
R middle temporal gyrus	41	-57	16	169
L insula	-33	19	4	165
L superior frontal gyrus	-23	49	28	123
L middle occipital gyrus	-29	-73	14	81
Seed: bilateral FEF				
L middle occipital gyrus	-27	-89	6	433
L cingulate gyrus	-3	15	28	138
R middle frontal gyrus	37	19	40	119
R insula	37	13	4	116
R thalamus	9	-7	20	84

Table S6. Human fMRI connectivity results. Related to Figure 7. Regions demonstrating greater connectivity with the seed region, during Go trials, compared with baseline.

Area	Talairach coordinates (mm)			Volume
	x	y	z	(mm^3)
Seed: ventral rVLPFC				
L inferior parietal lobule	43	-55	46	349
L middle frontal gyrus	-33	41	18	197
R superior parietal lobule	7	-49	62	118
R inferior parietal lobule	39	-55	46	113
L middle occipital gyrus	-29	-81	-8	108
R cingulate gyrus	3	1	48	87
R superior colliculus	1	-37	-10	84
Seed: bilateral FEF				
R insula	53	1	10	644
R superior colliculus	1	-33	-8	453
L insula	-33	5	18	262
L middle frontal gyrus	-39	43	24	175
L precentral gyrus	-51	-3	6	139
R inferior parietal lobule	51	-45	40	99
R precuneus	27	-71	36	80

Table S7. Human fMRI connectivity results. Related to Figure 7 Regions demonstrating greater connectivity with the seed region, during Continue trials, compared with baseline.

Area	Talairach coordinates (mm)			Volume
	x	y	z	(mm^3)
Seed: ventral rVLPFC				
L superior parietal lobule	-39	-57	48	331
L frontal eye field	-25	-9	50	144
L precentral gyrus	-33	3	28	106
L inferior parietal lobule	-49	-45	38	84
Seed: bilateral FEF				
R precuneus	5	-65	38	133

Table S8. Monkey electrophysiology results. Related to Figures 5 and 6. Recorded neuron types breakdown. Move: movement-related neurons. Visual: Visual neurons. VisMov: Visual-movement related neurons. Fix: fixation neurons. Ctx: neurons showing context-related activity. Other: neurons shown activities that were too complex to define for the purpose of the current study. Percent is calculated as the ratio between the number of neurons for each type and the total number of *task-related* neurons.

	Cell type							
Area	**Move**	**Visual**	**VisMov**	**Fix**	**Context-related**	**Other**	**Total task-related**	**Total recorded**
FEF	16	0	23	14	2	0	55	55
(%)	29.1	0.0	41.8	25.5	3.6	0.0		
rVLPFC	37	15	48	4	196	13	313	326
(%)	11.8	4.8	15.3	1.3	62.6	4.2		
Total	53	15	71	18	198	13	368	381